Nuclear Instruments and Methods in Physics Research A 596 (2008) 134–137

Contents lists available at ScienceDirect

Nuclear Instruments and Methods in Physics Research A

journal homepage: www.elsevier.com/locate/nima

First results of systematic studies done with silicon photomultipliers

C. Bosio [a], S. Gentile [b], E. Kuznetsova [a,*], F. Meddi [b]

[a] INFN Roma 1, Piazzale Aldo Moro 5, 00185 Roma, Italy
[b] Università degli Studi di Roma "La Sapienza", Piazzale Aldo Moro 5, 00185 Roma, Italy

ARTICLE INFO

Available online 29 July 2008

Keywords:
Silicon photomultiplier
Photon detection

ABSTRACT

Multicell avalanche photodiode structure operated in Geiger mode usually referred as silicon photomultiplier is a new intensively developing technology for photon detection. Insensitivity to magnetic fields, low operation voltage and small size make silicon photomultipliers very attractive for high-energy physics, astrophysics and medical applications.

The presented results are obtained during the first steps taken in order to develop a setup and measurement procedures which allow to compare properties of diverse samples of silicon photomultipliers available on market. The response to low-intensity light was studied for silicon photomultipliers produced by CPTA (Russia), Hamamatsu (Japan), ITC-irst (Italy) and SensL (Ireland).

1. Introduction

Silicon photomultiplier is a novel type of photodetectors with a multicell photodiode structure operating in the limited Geiger mode. The technology development started in 1990s [1,2] provided the photodetectors with a single photoelectron gain of about 10^6 and photodetection efficiency comparable with the one of vacuum photomultipliers. The same time the small size, capability to operate in a magnetic field, low bias voltage and reasonable price of the device induced a further intense development and enhancement of the technology leaded by different institutions and manufacturers [3–6]. This results in a number of different types of silicon photomultipliers available on market and produced by different manufacturers. Despite the different commercial names of the devices, here all of them are referred as SiPM.

Systematic studies done with various types of SiPM would provide start information for an optimal choice of the device appropriate for a given application. The results presented here are obtained during the first steps taken in order to develop a setup and measurement procedures which would allow to compare properties of diverse SiPM samples.

2. General principle of the SiPM operation

An SiPM consists of a large number of identical microcells with a common anode.

The microcells are located on a common substrate with a typical size of $\sim 1 \times 1\,\mathrm{mm}^2$. Fig. 1 shows a principal representation of the SiPM microcell structure. Under a reverse bias voltage U_{bias} above the breakdown value U_{brd}, the multilayer structure with different doping concentrations provides a high gradient of the electric field in the vicinity of the np-junction region. The electrons created via photoabsorption in the π-region drift toward the p layer where the avalanche multiplication occurs. The resistive layer on the top of the n-side provides a voltage drop during the avalanche development due to the growing current. This causes a redistribution of the potentials bringing the SiPM voltage down to the breakdown value U_{brd} when the avalanche is quenched. Thus the charge induced during the avalanche discharge is proportional to the overvoltage $Q = (U_{\mathrm{bias}} - U_{\mathrm{brd}}) \cdot C$, where C is the junction capacitance [3,7].

3. Measurement setup

The measurements discussed here include current–voltage characteristics and studies of the SiPM response to low-intensity light performed at room temperature. While results of the former measurements are mostly used to check the sample operability and to define the range of bias voltages for the latter studies, the measurements of the SiPM response to the light provide a number of parameters suitable for the comparison of different samples.

A principal scheme of the measurement setup is shown in Fig. 2. The bias voltage and current through an SiPM sample are monitored in the voltage circuit. The SiPM is illuminated with light from a light emitting diode operated in a pulse mode. The signal from SiPM is read out with a charge-sensitive preamplifier and digitised with an integrating ADC. The LED pulse of about 6 ns

* Corresponding author.
E-mail address: Ekaterina.Kouznetsova@roma1.infn.it (E. Kuznetsova).

0168-9002/$ - see front matter © 2008 Published by Elsevier B.V.
doi:10.1016/j.nima.2008.07.135

duration and ADC gate of about 100 ns width are synchronised by means of a common trigger.

The measurements are done at room temperature. Temperature variation during the measurements done for one sample did not exceed 2 °C, for all measurements discussed here the total variation was less than 4 °C.

Fig. 3 shows an example of the SiPM response to low-intensity light measured with the described setup. The spectrum is obtained with a CPTA produced device distributed by Obninsk University (Russia). The peaked structure indicates the number of cells fired during one light pulse, starting with the pedestal for no cells fired. The distance between adjacent peaks corresponds to the SiPM gain.

The spectrum is fitted as a sum of Gaussian distributions:

$$\sum_i G(N_i, \mu_i, \sigma_i) = \sum_i G(N_i, \mu_0 + i \cdot g, \sigma_i) \quad (1)$$

where μ_0 is the pedestal position and g is the gain in units of ADC counts.

From statistical considerations the width of i th peak σ_i can be expressed as

$$\sigma_i = \sqrt{\sigma_0^2 + i \cdot \langle\sigma_{px}\rangle^2} \quad (2)$$

where σ_0 is the pedestal width and $\langle\sigma_{px}\rangle$ represents fluctuations of the one-cell response averaged over the active area of the sample.

In order to check reproducibility of the measurements and fitting procedures, a series of spectra was taken for the same bias voltage but under different light intensities. Fig. 4 shows the fitted width of i th peak obtained from different measurements (top) and the corresponding averaged values (bottom) as functions of the peak number. The latter dependence is fitted according to Eq. (2).

Fig. 5 shows the gain as a function of the bias voltage U_{bias} obtained for the CPTA/Obninsk sample. The breakdown voltage U_{brd} is defined here as the bias voltage corresponding to the gain equal to one and is found from the linear fit to be equal 44.99 ± 0.13 V.

The width of the spectrum peaks described by Eq. (2) increases with the bias voltage. The dark current significantly increases with overvoltage and thus causes the pedestal broadening. The same time, fluctuations of the signal from one single cell increases with voltage due to the increasing gain:

$$\sigma_{px} = \sqrt{N} \quad (3)$$

where N is the average number of charge carriers in the avalanche. However, being averaged over the active area of SiPM, $\langle\sigma_{px}\rangle$ contains also a systematic part:

$$\langle\sigma_{px}\rangle \sim \sqrt{N + \sigma_{\text{nu}}^2} \quad (4)$$

where σ_{nu} represents non-uniformity of the amplification over the SiPM active area.

To characterise the dependence of SiPM signal properties on the overvoltage, the ratios of the gain to the values of σ_0 and $\langle\sigma_{px}\rangle$ were studied. Fig. 6 shows an example of the dependence obtained for the discussed sample.

For SiPM the gain is equal to the average number of charge carriers in the avalanche, $g = N$, so the ratio $g/\langle\sigma_{px}\rangle$ tends to a linear behaviour for the low gain values $N \ll \sigma_{\text{nu}}^2$. For the high gain values $N \gg \sigma_{\text{nu}}^2$ the dependence would correspond to square root low $g/\langle\sigma_{px}\rangle \sim \sqrt{N}$ in the case of a constant σ_{nu}. Such a behaviour is seen in Fig. 6.

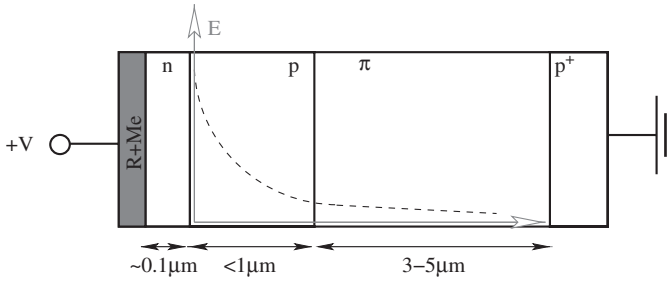

Fig. 1. Principal representation of an SiPM microcell.

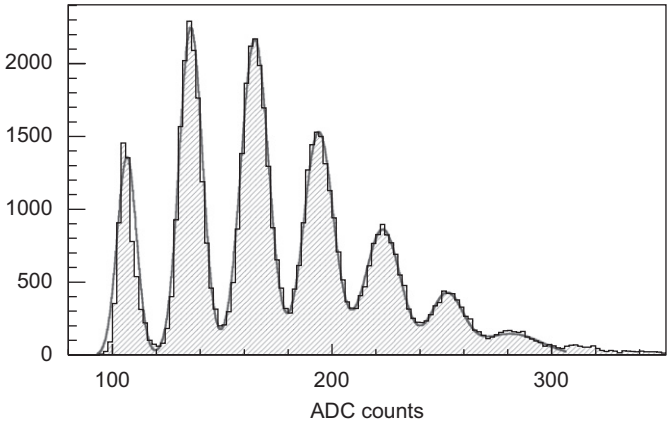

Fig. 3. ADC spectrum of the SiPM response to the low-intensity pulsed light (dashed histogram) fitted to a superposition of seven Gaussian peaks (grey line). The spectrum is obtained with a CPTA produced device distributed by Obninsk University (Russia).

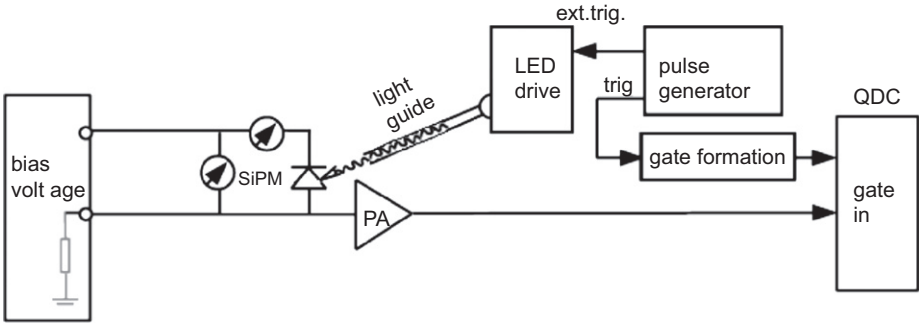

Fig. 2. A principal scheme of the measurement setup. The bias voltage and current through an SiPM sample are monitored in the voltage circuit. The SiPM is illuminated with light from a light emitting diode (LED) operated in a pulse mode. The signal from SiPM is read out with a charge-sensitive preamplifier (PA) and digitised with an integrating ADC. The LED pulse and ADC gate are synchronised by means of a common trigger.

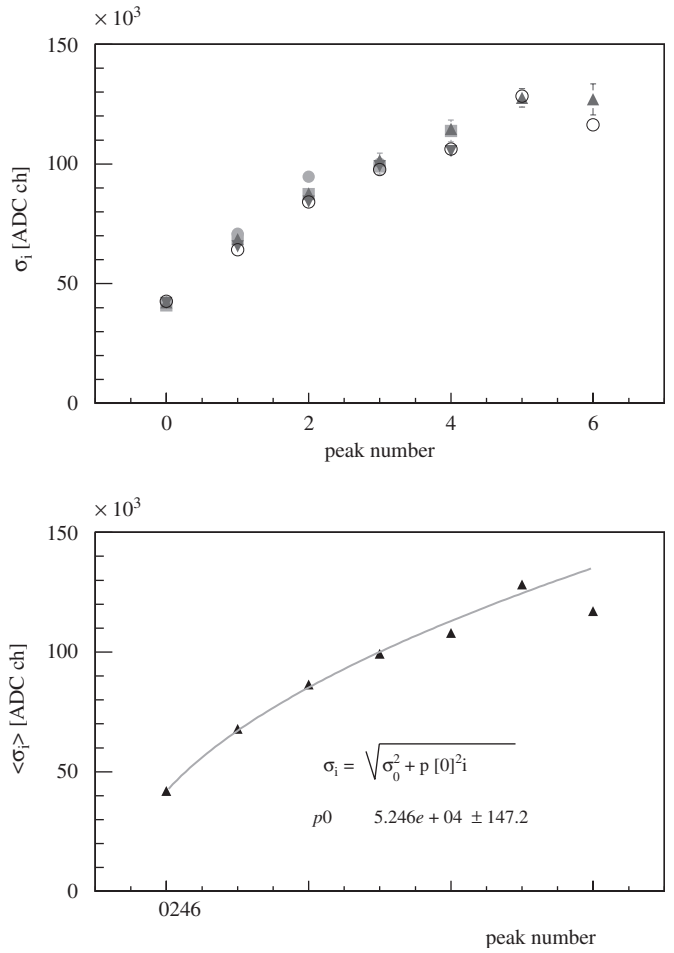

Fig. 4. Fit values for the width of *i* th peak as a function of the peak number (top). The results obtained from different measurements are shown with different markers. The corresponding averaged values as a function of the peak number (bottom) are fitted according to Eq. (2).

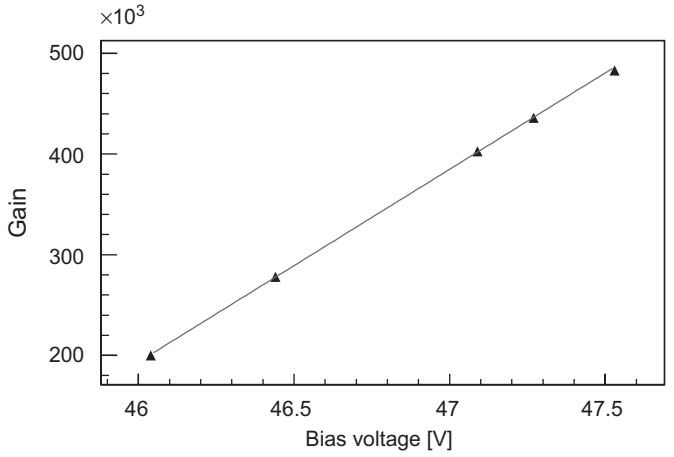

Fig. 5. Gain as a function of the bias voltage obtained for the CPTA/Obninsk sample.

4. Comparison of different samples

Five samples of silicon photomultipliers have been studied. CPTA[1] produced samples distributed by Obninsk University and Forimtech,[2] HAMAMATSU produced Multi-Pixel Photon Counter S10362-11-025C [8], ITC-irst[3] sample produced in the second production run on May 2006 and SensL[4] SPMScint sample were compared on the base of the measurement results. Table 1 summarises basic characteristics of the listed SiPMs.

[1] CPTA, Russia, http://www.zao-cpta.ru.

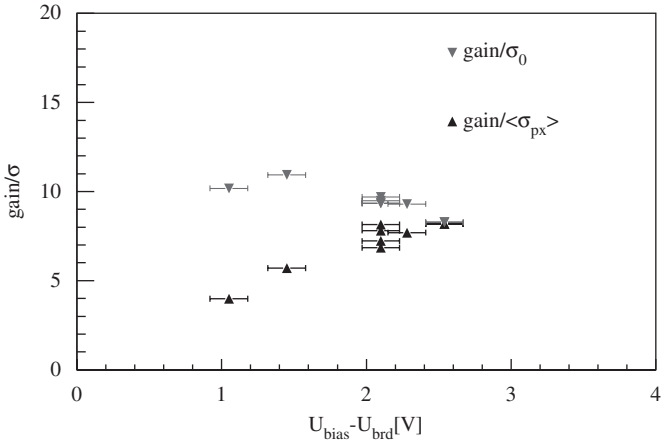

Fig. 6. The gain normalised to the corresponding values of pedestal width and $\langle\sigma_{px}\rangle$ as functions of the overvoltage obtained for the CPTA/Obninsk sample.

Table 1
Basic characteristics of the studied SiPMs

	Number of cells	Cell size (μm²)	Fill factor
CPTA/Forimtech[a]	~550	~43 × 43	
CPTA/Obninsk[a]	~550	~43 × 43	
HAMAMATSU	1600	25 × 25	0.31
ITC-irst	625	40 × 40	~0.2
SensL	520	35 × 35	0.60

The active area of all samples is 1 mm².
[a] Measured values.

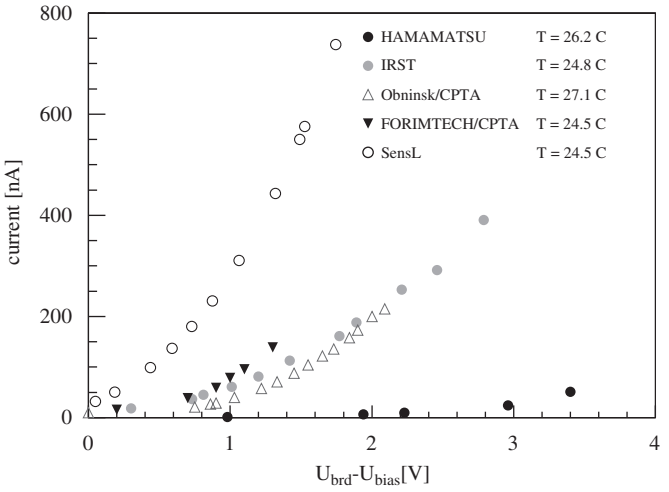

Fig. 7. The current–voltage characteristics measured for the studied samples.

[2] Forimtech SA, http://www.forimtech.ch.
[3] ITC-irst, Italy, http://www.itc.it/irst.
[4] SensL, Ireland, http://www.sensl.com.

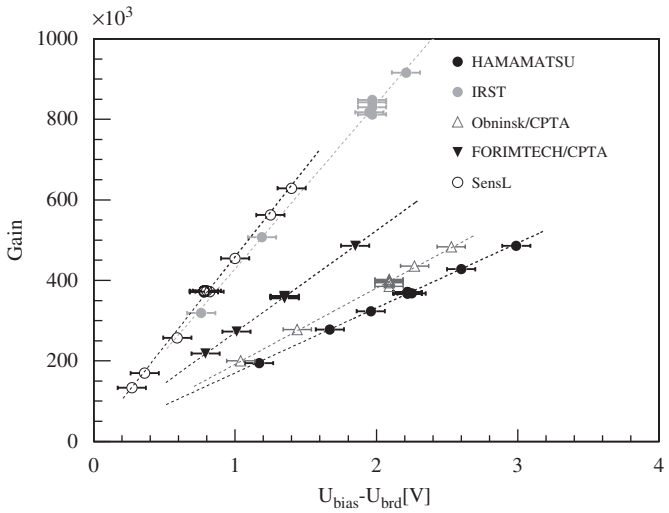

Fig. 8. Gain as a function of the overvoltage.

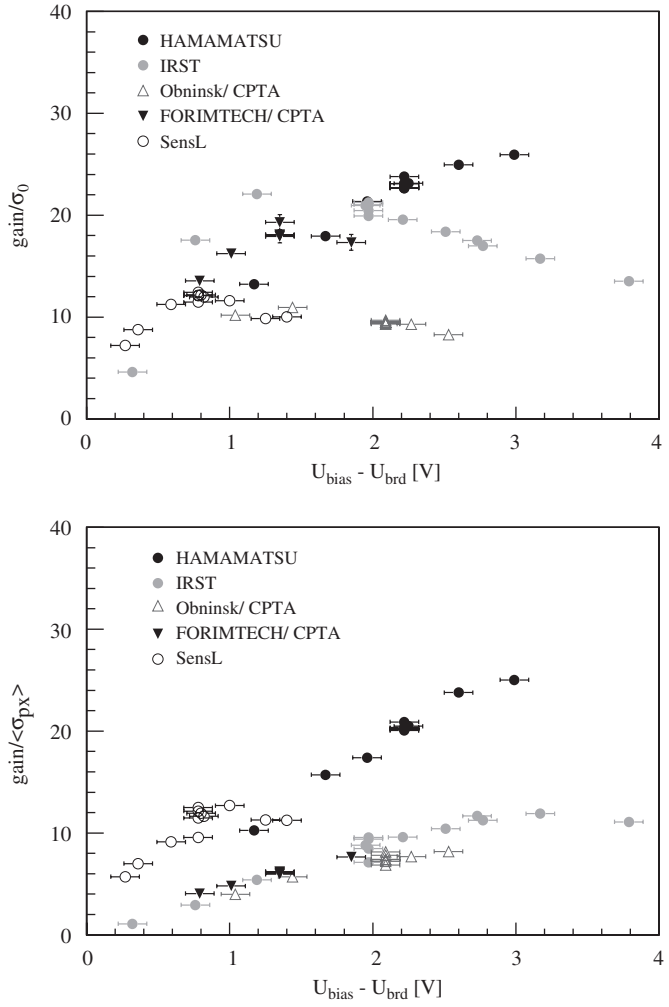

Fig. 9. The gain normalised to the corresponding values of pedestal width (top) and $\langle\sigma_{px}\rangle$ (bottom) as functions of the overvoltage.

Fig. 7 shows the current–voltage characteristics. The gain as a function of the overvoltage is shown in Fig. 8.

Fig. 9 shows the ratios of the gain to the values of σ_0 (top) and $\langle\sigma_{px}\rangle$ (bottom) obtained for the studied sample. As it was mentioned above, for the constant non-uniformity factor σ_{nu} the ratio $g/\langle\sigma_{px}\rangle$ is expected to increase with overvoltage following the linear or square root low. However, as seen from Fig. 9 (bottom), the ratio obtained for some of the samples shows tendency to a slower increase, what indicates a growth of the non-uniformity factor σ_{nu} with the overvoltage.

5. Conclusion

The obtained results demonstrated operability and potential of the developed setup. Further development and tune of the setup, measurement procedure and data treatment will allow to obtain comparative characteristics of diverse types of silicon photomultipliers.

Acknowledgements

We would like to thank Prof. R. Battiston (University and INFN of Perugia), Prof. V. Saveliev (Obninsk State University and DESY), Dr. I. Polak (Institute of Physics of the ASCR, Prague), Dr. E. Popova (MEPhI) and Mr. N. D'Ascenzo (DESY) for their support and fruitful discussions.

References

[1] G. Bondarenko, et al., Nucl. Phys. Proc. Suppl. 61B (1998) 347.
[2] P. Buzhan, et al., Nucl. Instr. and Meth. A 504 (2003) 48.
[3] V. Golovin, V. Saveliev, Nucl. Instr. and Meth. A 518 (2004) 560.
[4] B. Dolgoshein, et al., Nucl. Instr. and Meth. A 563 (2006) 368.
[5] K. Yamamoto, et al., IEEE Nucl. Sci. Symp. Conf. Rec. 2 (2006) 1094.
[6] N. Dinu, et al., Nucl. Instr. and Meth. A 572 (2007) 422.
[7] C. Piemonte, Nucl. Instr. and Meth. A 568 (2006) 224.
[8] Hamamatsu Photonics K.K, Product catalogue No. KAPD0002E02, 2007.